IEEE Access
Multidisciplinary | Rapid Review | Open Access Journal

Received June 8, 2019, accepted June 21, 2019, date of publication June 27, 2019, date of current version July 18, 2019.

Digital Object Identifier 10.1109/ACCESS.2019.2925389

A Novel Bandwidth-Enhanced Dual-Polarized Antenna With Symmetrical Closed-Resonant-Slot Pairs

SUIDAO FU, ZHENXIN CAO, PENG CHEN, DI GAO, XIN QUAN
School of Information Science and Engineering, Southeast University, 210096 Nanjing, China

Corresponding author: Zhenxin Cao (caozx@seu.edu.cn)

This work was supported in part by the National Natural Science Foundation of China under Grant 61471117 and Grant 61801112 and in part by the Fundamental Research Funds for the Central Universities under Grant 2242019k1G002.

ABSTRACT A novel bandwidth-enhanced dual-polarized antenna (BEDPA) with symmetrical closed-resonant-slot pairs for 2/3/4G and international mobile telecommunications bands is proposed. The BEDPA is realized by etching closed slots symmetrically on the conventional cross-dipole broadband dual-polarized antenna to increase a new resonant mode in the higher band. As simulation and experiment indicated, the BEDPA obtains an impedance bandwidth of 67.3% (1.4 − 2.82 GHz) for VSWR < 1.5, which is 11.5% wider than the conventional cross-dipole broadband dual-polarized antenna, and a high port-to-port isolation (ISO) > 38 dB. Over the operating frequency, the BEDPA achieves a stable radiation pattern with a half-power beamwidth (HPBW) within 64.5 ± 4.5°, a gain within 8.9 ± 0.7 dBi, and a cross-polarization discrimination (XPD) > 22 dB. Furthermore, a linear array with an impedance bandwidth of 73.1% (1.37 − 2.95 GHz) and an ISO > 27 dB is fabricated for the active antenna unit application. The linear array achieves a HPBW within 64 ± 6.5°, a gain within 16.5 ± 1.5 dBi, a sidelobe suppression (SLS) > 16 dB, and a front-to-back ratio (F/B) > 24 dB.

INDEX TERMS Bandwidth enhancement, dual-polarized antenna, multiple resonant modes, closed resonant slot.

I. INTRODUCTION

The broadband dual-polarized antennas have been proposed for 2/3/4G bands (1.71 − 2.69 GHz) [1]–[12], and widely used to boost channel capacity in the base stations for mobile communication by reducing multipath effects. At the international radio communication conference of international telecommunication union (ITU) in 2015, 1.427 − 1.518 GHz was defined as the globally uniform frequency of international mobile telecommunications (IMT) to meet an increasing demand for both wireless communications and outdoor signal coverage. Therefore, it is important to develop a dual-polarized antenna for 1.427 − 2.69 GHz.

Bandwidth-enhanced dual-polarized antennas (BEDPAs) with operating bandwidth from1.427 to 2.69 GHz have just been proposed in the last year. In [13], Cui *et al.* proposed a four-leaf clover BEDPA covering 1.39 − 2.8 GHz, where U-shaped slots to radiator were used to shorten the current path for high frequency and a parasitic element of four disks above the radiator were used to change the impedance matching. However, the antenna structure is complicated and the feeding method is difficult to solder. Zhang *et al.* has proposed a compact dual-polarized antenna to achieve a bandwidth of 68% (1.427 − 2.9 GHz) [14], where its radiator is designed as the spline-edged bowties and fed by tapered impedance matching lines. However, the port-to-port isolation (ISO) is only 20 dB. Reference [15] has proposed two types of BEDPAs. Type I introduced a parasitic loop below two crossed dipoles and a parasitic disk with four parasitic strips above to achieve a wide frequency band of 64% (1.4 − 2.75 GHz) with an ISO being 30 dB, but the antenna size is $0.93\lambda_0 \times 0.93\lambda_0 \times 0.38\lambda_0$ (λ_0 is the wavelength corresponding to 2.1 GHz in free space). Type II was composed of a pair of perpendicularly crossed dual parallel dipoles. To achieve enhanced bandwidth 1.4 − 2.7 GHz, a parasitic circular disk was introduced above the cross-dipole elements. However, Type I is limited by larger size and complex structure, while Type II has an unstable radiation pattern due to the orthogonal component of the surface current.

An ultra-wideband notch antenna is proposed in [16] by etching a half wavelength slot on the antenna to generate

The associate editor coordinating the review of this manuscript and approving it for publication was Hassan Tariq Chattha.

 This work is licensed under a Creative Commons Attribution 3.0 License. For more information, see http://creativecommons.org/licenses/by/3.0/

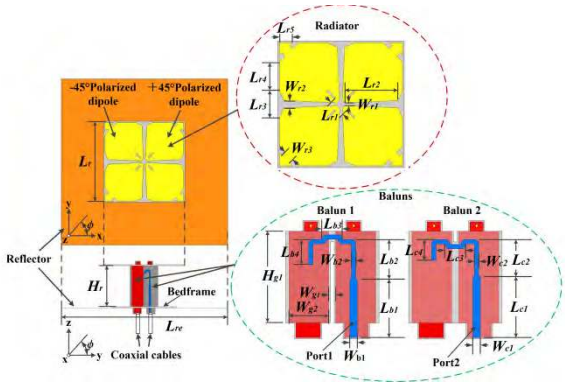

FIGURE 1. Configuration of the cross-dipole broadband dual-polarized antenna.

a resonant mode. It is also an effective method to broaden the input impedance by generating a new resonant mode for cross-dipole broadband dual-polarized antenna. In this paper, a high-performance BEDPA with symmetrical closed-resonant-slot pairs is proposed. An enhanced bandwidth from 1.40 GHz to 2.82 GHz with VSWR < 1.5 is realized, where closed resonant slots symmetrically etched on the cross-dipole broadband dual-polarized antenna to generate a new resonant mode. The fundamental principle is described in section II. The BEDPA element and a linear array are presented in section III. The conclusion is demonstrated in section IV.

II. OPERATING PRINCIPLE

A. DUAL-POLARIZED ANTENNA CONFIGURATION

As illustrated in Fig. 1, a conventional cross-dipole broadband dual-polarized antenna designed consists of a radiator, two baluns, a bedframe and a reflector. The radiator is fixed to the bedframe by the perpendicularly crossed baluns, and the reflector is placed below the bedframe. The radiator consists of a pair of orthogonal crossed dipoles which are printed on the upper surface of the substrate (relative dielectric constant $\varepsilon_r = 2.66$ and thickness $= 1$ mm, same as below). One dipole is for $+45°$ polarization and the other is for $-45°$ polarization. In order to achieve a better impedance matching, the gap between the adjacent dipole arms is designed as a two-step structure in both different widths. At the same time, an arrow-shape patch is designed at the both end of the dipole arms. Therefore, the arm shape of the dipole is a combination of diamond-shape and arrow shape. The configuration of the baluns is similar to that in [5]. The height of balun is 35.5 mm ($0.25\lambda_0$). With a Γ-shaped feeding line printed on the front side and two patches on the back side, a substrate is contributed to the main structure of the balun. Γ-shaped feeding line is connected with 50 Ω coaxial cables, and the patches are electrically connected to the radiator and ground plane of the bedframe. Balun-feeding structure contributes to achieve a high ISO than the conventional coaxial feed for antenna. Port 1 is connected to the balun 1 for the $+45°$ polarization feed, and port 2 is connected to the balun 2 for the $-45°$ polarization feed.

TABLE 1. The parameters of cross-dipole broadband dual-polarized antenna (unit: mm).

Parameter	Value	Parameter	Value	Parameter	Value
H_r	35.5	W_{r2}	4.26	L_{c2}	13.8
L_{re}	170	W_{r3}	6	L_{c3}	7.6
L_r	71	L_{b1}	22	L_{c4}	7.8
L_{r1}	10	L_{b2}	14.8	W_{c1}	2.7
L_{r2}	30.4	L_{b3}	7.6	W_{c2}	1.6
L_{r3}	15.3	L_{b4}	9.3	W_{g1}	2.5
L_{r4}	16.9	W_{b1}	2.7	W_{g2}	15
L_{r5}	7.5	W_{b2}	1.6	H_{g1}	34.5
W_{r1}	1.64	L_{c1}	23		

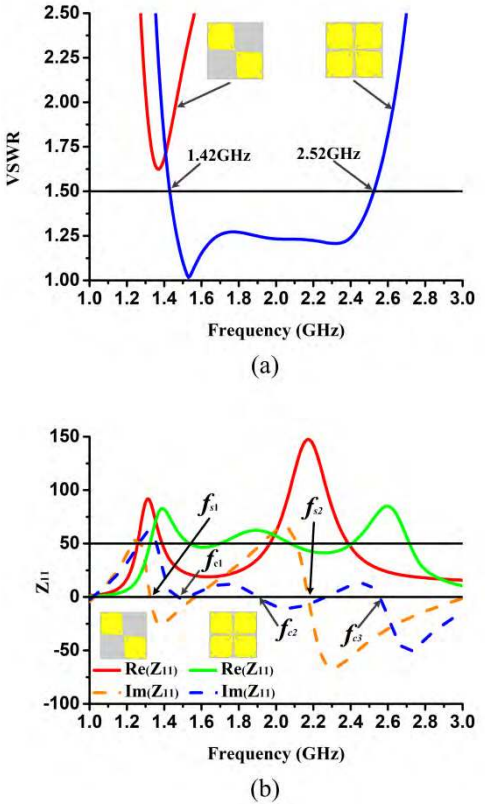

FIGURE 2. (a) VSWR and (b) Input impedance of the single-dipole/cross-dipole broadband dual-polarized antenna.

The dual-polarized antenna is simulated and optimized by Ansoft HFSS 15, and the geometric parameters are given in Table 1. As shown in Fig. 2(a), the antenna has an impedance bandwidth 55.8% from 1.42 GHz to 2.52 GHz (only port 1 is excited due to the symmetry of the structure), and similar to the other cross-dipole broadband dual-polarized antennas [3]–[5], [7], [9], [17].

B. DESIGN PRINCIPLE

First, it is necessary to consider the input impedance of the dual-polarized antenna. The conventional cross-dipole broadband dual-polarized antennas for base station produce

multiple resonant modes in the band. An ideal dipole is placed at a 0.25λ from the infinity ground plane. The input impedance can be calculated by the mirror principle [18]:

$$Z_{in} = \frac{R_r}{\sin^2 \beta l} - jZ_a \cos \beta l \tag{1}$$

where

$$R_r = R_{11} + R_{12} \tag{2}$$

$$Z_a = 120(\ln \frac{2l}{\rho} - 1) \tag{3}$$

$$\beta = \lambda_a \frac{2\pi}{\lambda} \tag{4}$$

where, l is half the length of the dipole, ρ is the radius of the dipole. R_{11} is the self-resistance of dipole, R_{12} is the mutual resistance between the mirror dipole and the original one, Z_a is the characteristic impedance between the two arms of the dipole and λ_a is the wavelength on the dipole. Due to the coupling between the crossed dipoles, the input impedance of the cross-dipole placed on the ground plane is generally obtained by numerical calculation. Fig. 2 shows the input impedance and VSWR of the single-dipole/cross-dipole broadband dual-polarized antenna mentioned above. As illustrated in Fig. 2(b), for the single-dipole, it has two resonant modes: the first resonant frequency f_{s1} is depended on the maximum aperture of the dipole; the second frequency f_{s2} is generated by the impedance transformation of balun feeds. For the cross-dipole, it has 3 resonate modes: the production mechanism of the first and second resonate frequency f_{c1}, f_{c2} is the same as the single-dipole, and the third resonant frequency f_{c3} is generated by the coupling between adjacent crossed dipoles. The resistance and reactance of Z_{11} fluctuates around 50 Ω and 0 from f_{c1} to f_{c3}, respectively. As the frequency increasing, the reduced resistance and increased reactance produce a stopband around 2.8 GHz.

The closed resonant slot can be studied by slot antenna placed on the ground plane. According to the Booker relation, the input impedance of slot on a large-sized conductor plate is [18]:

$$Z_{in}^s = \frac{(60\pi)^2}{Z_{in}^d} \tag{5}$$

where Z_{in}^d is input impedance of the dipole complementary to the slot. For the half-wave slot, the input reactance is zero. Fig. 3(a) shows the input impedance of the angular slot antenna. Compared to other conventional slots like liner slot and H-shape slot, the angular slot successfully saves size due to bending, and greatly avoids the research difficulty caused by complicated structure. The angular slot antenna has a resonant frequency at 2.8 GHz with a length of 43.6 mm ($0.41\lambda_{2.8GHz}$, $L_{a1} = 17.1$ mm). The resonant current distribution is also shown in Fig. 3. It is found that the strongest current is generated at both ends of the angular slot, and the zero current is generated at the middle of the angular slot.

As the closed resonant slots etched on the cross-dipole broadband dual-polarized antenna, it is desirable to reduce the

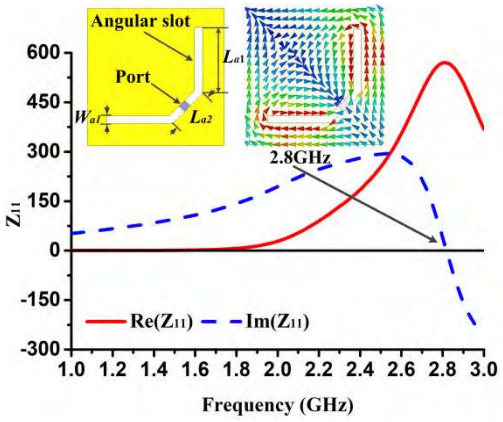

FIGURE 3. Input impedance and resonant current distribution. (unit: mm, $W_{a1} = 2$, $L_{a1} = 17.1$, $L_{a2} = 9.4$).

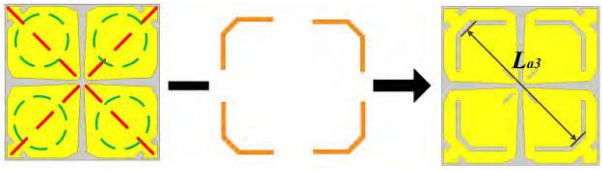

FIGURE 4. Configuration of the BEDPA. (unit: mm, $L_{a3} = 71.5$).

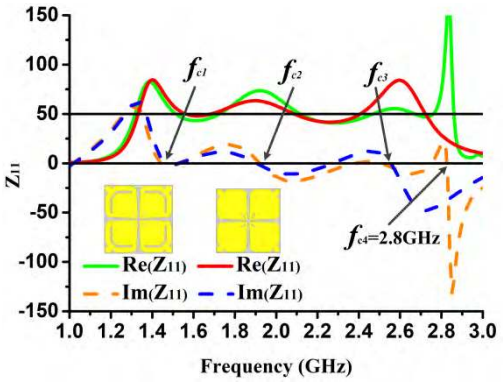

FIGURE 5. Input impedance of the BEPDA with/without angular slots.

effect on the current distribution in the lower band. The main current flows along the edge of the cross-dipole patch and is weakest at the middle of the patch. Therefore, the BEDPA is achieved by symmetrically placing four angular slots at the ends of the crossed dipole axis, and making the center of the slot be toward central axis of the antenna. Fig. 4 shows the BEDPA design process. The red dashed line is the axis of the dipole and the green dashed line is the weakest current distribution on the dipole. The BDEPA is obtained by etching four angular slots on the radiator patch. The input impedance of the BEDPA with/without angular slots are illustrated in Fig. 5. There is no significant difference on the input impedance of the BEDPA with/without angular slots at the lower band. As angular slots introduced, a new resonant mode f_{c4} appears at the 2.8 GHz. The input impedance has changed in the high frequency, and a passband is generated at 2.72 GHz.

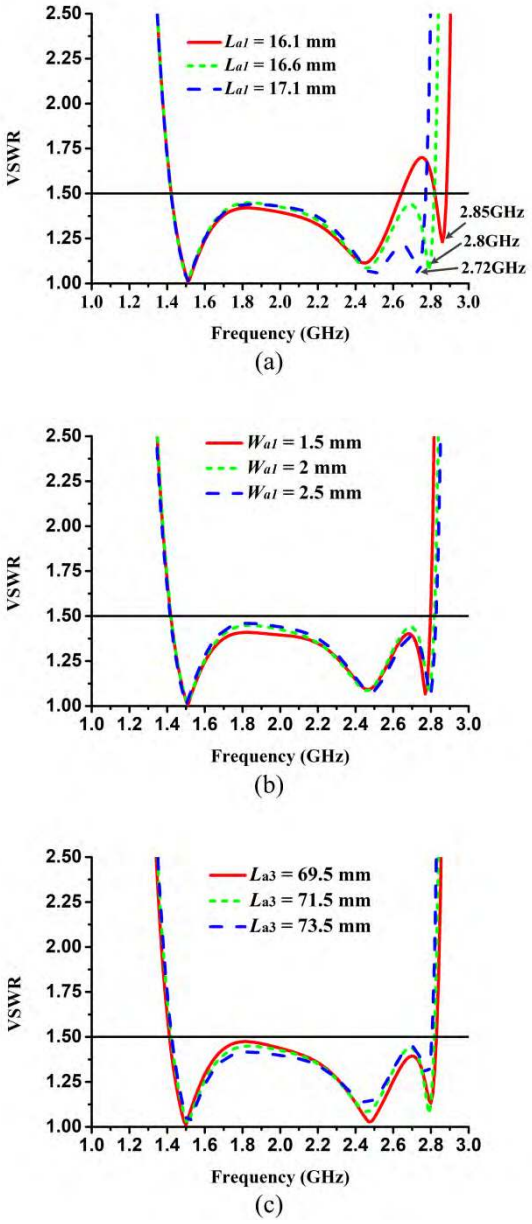

FIGURE 6. Effect of the (a) length (L_{a1}), (b) width (W_{a1}) and (c) position (L_{a3}) on VSWR of the BEDPA for the angular slots.

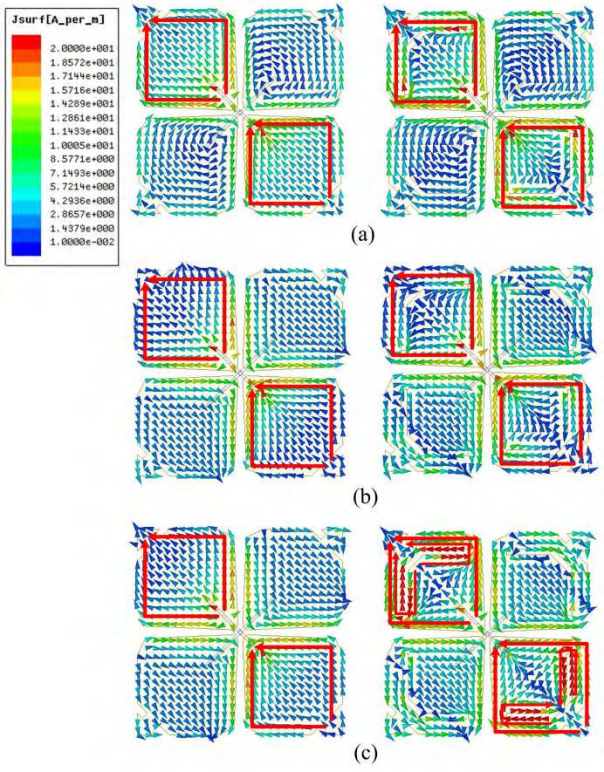

FIGURE 7. Current distribution of the BEDPA with/without angular slots at (a) 1.5, (b) 2.4, and (c) 2.8 GHz.

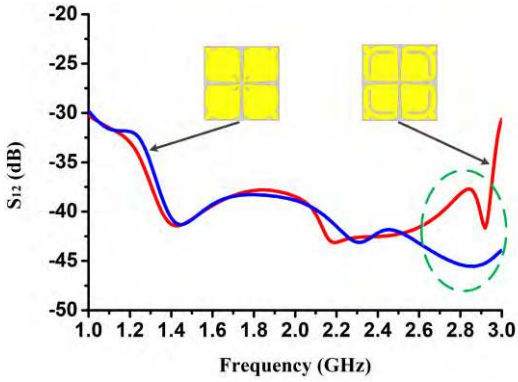

FIGURE 8. ISO of the BEDPA with/without angular slots.

The effect of the length (L_{a1}) on the VSWR of the BEDPA for the closed resonant slots is exhibited in Fig. 6(a). As the length shortens, the passband moves higher. When the length is 42.6mm ($0.4\lambda_{2.8GHz}$, L_{a1} = 16.6 mm), a passband is generated at 2.8 GHz, and the BEDPA obtains an impedance bandwidth from 1.42 to 2.82 GHz with VSWR < 1.5. The effect of the width (W_{a1}) on the VSWR for the closed resonant slots is shown in Fig. 6(b). The VSWR is not significantly influenced by the width changes when the width is much smaller than this length. The effect of the position (L_{a3}) on the VSWR for the closed resonant slots is demonstrated in Fig. 6(c). The position of the angular slots affects the impedance matching in the new passband. The optimal value L_{a3} is 71.5 mm.

For a better understanding, Fig. 7 shows the current distribution of BEDPA with/without closed resonant slots at 1.5, 2.4 and 2.8 GHz. At 1.4 and 2.4 GHz, there is no significant change in current distribution with/without closed resonant slots. At 2.8 GHz, there is a resonant current on the edge of the slots as the angular slots be introduced.

C. PERFORMANCE ANALYSIS

The VSWR is required to meet the requirements, and ISO and radiation pattern is also expected to have superior performance for a high-performance dual-polarized antenna. The ISO of the BEDPA with/without angular slots exhibited in Fig. 8. The ISO is significant deteriorated form

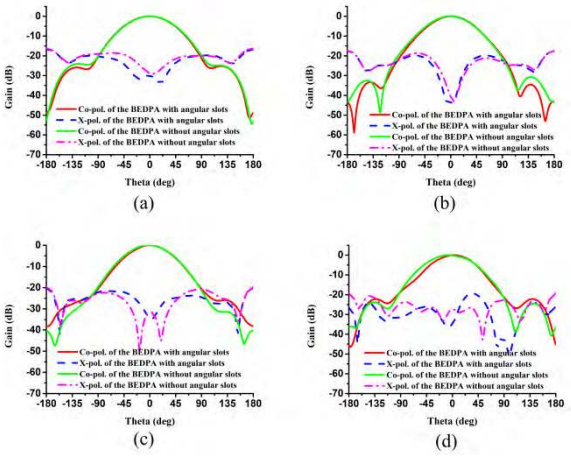

FIGURE 9. Radiation pattern of the BEDPA with/without ORS at (a) 1.42, (b) 1.9, (c) 2.4, and (d) 2.7 GHz.

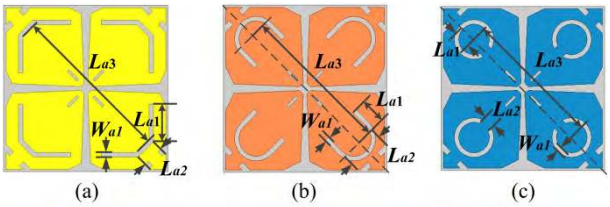

FIGURE 10. Three different closed resonant slots (a) angular slot, (b) U-shaped slot, and (c) C-shaped slot.

TABLE 2. The parameters of different closed resonat slots (unit: mm).

Parameter	Angular slot	U-shaped slot	C-shaped slot
W_{a1}	2	2	2
L_{a1}	16.6	8.4	8.9
L_{a2}	9.4	8.7	5
L_{a3}	71.5	61.5	61.5

45 dB to 37 dB around 2.8 GHz due to the angular slots destroy the orthogonality of the radiation current at the resonant frequency. The radiation pattern of the BEDPA with/without angular slots in the horizontal plane (*zox*-plane) for +45° polarization is shown in Fig. 9. There is no significant change on radiation pattern as the angular slots etched at the lower band. The beam squint of BEDPA from −6.5° to 3.5°, and the cross-polarization at the main lobe is increased after the angular slots etched at 2.7 GHz. This phenomenon is caused by the closed resonant slots changing the radiation current path at the high frequency. Reducing the physical size of the closed resonant slots mitigates this change on radiation pattern. In general, high ISO and stable radiation pattern can be guaranteed by appropriate selection of closed resonant slots parameters.

According to the method above, the BEDPAs with three different types of the closed resonant slot are shown in Fig. 10, and the geometric parameters are given in Table 2.

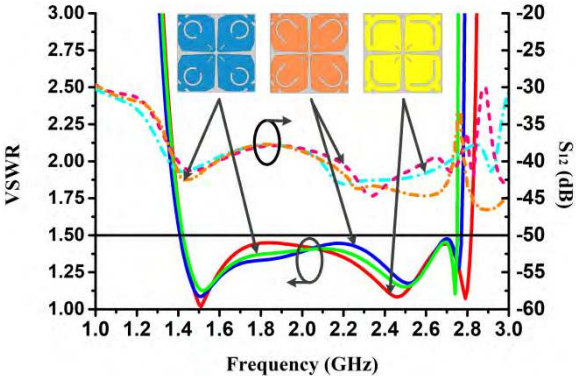

FIGURE 11. The VSWR and ISO of the BEDPA with different closed resonant slots.

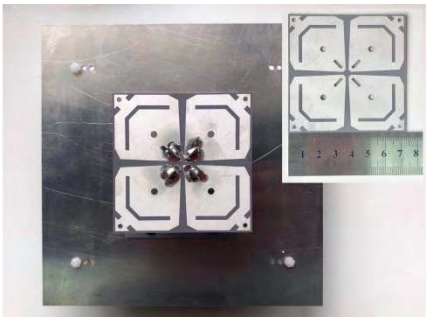

FIGURE 12. Prototype of the BEDPA.

The VSWR and ISO of the BEDPA with different closed resonant slots are demonstrated in Fig. 11. It is found that a passband is generated at 2.72 GHz for C-shaped slots with a length of 44.6 mm ($0.4\lambda_{2.72\text{GHz}}$), and a passband is generated at 2.75 GHz for U-shaped slots with a length of 44.1 mm ($0.4\lambda_{2.75\text{GHz}}$). The BEDPAs with 3 different closed resonant slots obtain an enhanced bandwidth covering 1.42 to 2.69 GHz with VSWR < 1.5, and an ISO > 30 dB. It should be noted that different types of the closed resonant slots have different Q values, so the new passband bandwidth is different. It should be noted that the BEDPA with angular slot increases bandwidth by 11.5% compared to the original dual-polarized antenna (1.42 − 2.52 GHz). The simulation data demonstrates that introducing symmetrical closed-resonant-slot pairs on the cross-dipole dual-polarized antenna creates a new resonant mode for bandwidth enhancement.

III. EXPERIMENTAL RESULTS

A. BEDPA ELEMENT

The prototype of the fabricated BEDPA with angular slots is shown in Fig. 12. There are four holes in the middle of the antenna to fix the radiator by plastic columns, and four holes at the top corner to weld metal screws if VSWR shift toward high frequency. All the holes have no effect on the performance of the antenna. As illustrated in Fig. 13(a), a good agreement is observed between the measured results and the simulation for VSWR and ISO. A passband appears at the design frequency of 2.8 GHz. It can be seen that the

TABLE 3. Comparisons of bandwidth-enhanced dual-polarized antennas.

Ref	Bandwidth	ISO	HPBW	Gain	Antenna size
[19]	68% (RL > 10dB)	> 20 dB	66.8 ± 3.4°	7.7 ± 1.7 dBi	$0.5\lambda_0\times0.5\lambda_0\times0.263\lambda_0$
[14]	68% (VSWR < 1.5)	> 20 dB	65 ± 11°	8.5 ± 2 dBi	$0.54\lambda_0\times0.54\lambda_0\times0.24\lambda_0$
[15] Type I	64% (RL > 15dB)	> 30 dB	70 ± 8°	9 ± 0.6 dBi	$0.93\lambda_0\times0.93\lambda_0\times0.38\lambda_0$
[15] Type II	63% (RL > 15dB)	> 30 dB	60 ± 10°	8.6 ± 1.2 dBi	$0.68\lambda_0\times0.68\lambda_0\times0.38\lambda_0$
[13]	67% (RL > 15dB)	> 30 dB	65 ± 5°	8.5 ± 0.7 dBi	$0.464\lambda_0\times0.464\lambda_0\times0.35\lambda_0$
This work	67.3% (VSWR < 1.5)	> 38 dB	64.5 ± 4.5°	8.9 ± 0.7 dBi	$0.49\lambda_0\times0.49\lambda_0\times0.248\lambda_0$

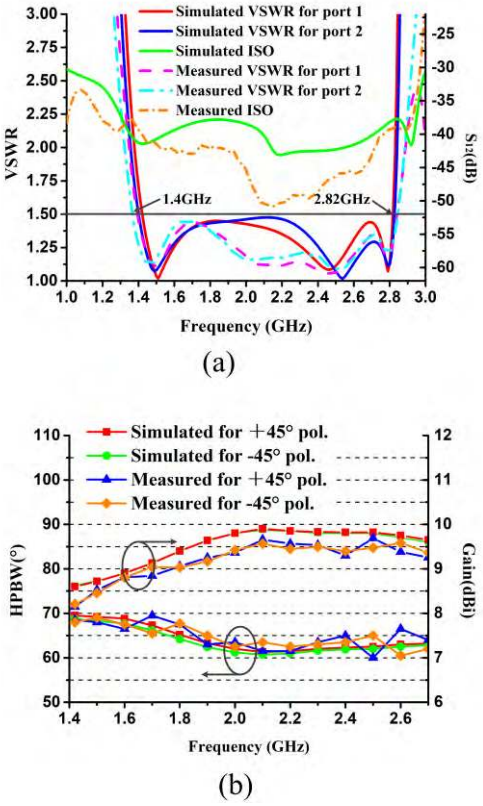

FIGURE 13. Measured and simulated (a) VSWR and ISO and (b) Gain and HPBW of the BEDPA.

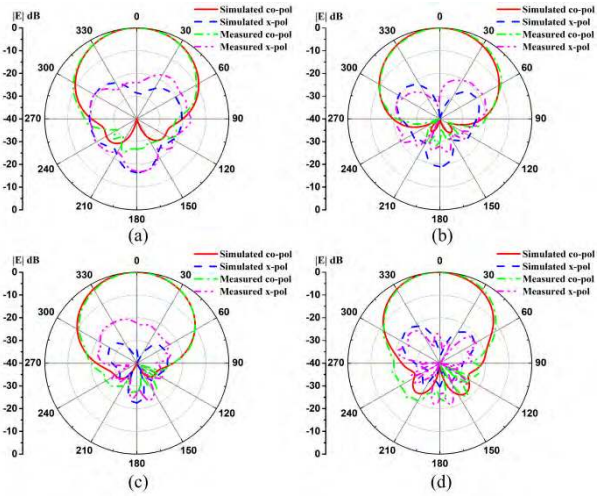

FIGURE 14. Radiation patterns of the BEDPA at (a) 1.42, (b) 1.9, (c) 2.4, and (d) 2.7 GHz.

FIGURE 15. Prototype of linear array with the BEDPA.

BEDPA achieves a bandwidth of 67 % (1.4 − 2.82 GHz) for VSWR < 1.5 and an ISO > 38 dB. Fig. 13(b) shows the gain and half-power beamwidth (HPBW) in the *zox*-plane for both two polarizations. The gain is 8.9 ± 0.7 dBi and the HPBW is 64.5 ± 4.5°. The radiation patterns at 1.42, 1.9, 2.4 and 2.7 GHz for +45° polarization are shown in Fig. 14. The simulated and measured patterns agree well. The measured cross-polarization discrimination (XPD) is >22 dB at the main lobe in *zox*-plane. To illustrate the advantages of the BEDPA proposed in this paper, Table 3 shows the detailed comparisons between other BEDPAs reported in recently years (the antenna size without the reflector). It is found that the BEDPA proposed has the advantages of high ISO, stable radiation pattern, compact size and simple construction. It is suitable for manufacturing active antenna unit in 2/3/4G and IMT bands.

B. BEDPA ARRAY

To verify the commercial value of the antenna proposed, a prototype of the linear array with BEDPA is shown in Fig. 15.

To meet the AAU requirements that the sidelobe level suppression (SLS) is greater than 15 dB and the gain is greater than 15.5 dBi, the spacing of adjacent elements is set to be 110 mm ($0.77\lambda_0$) and the number of elements is chosen to be 8. An eight-way Chebyshev power divider with VSWR < 1.3 (1.2 − 3.0 GHz) is designed for feed the

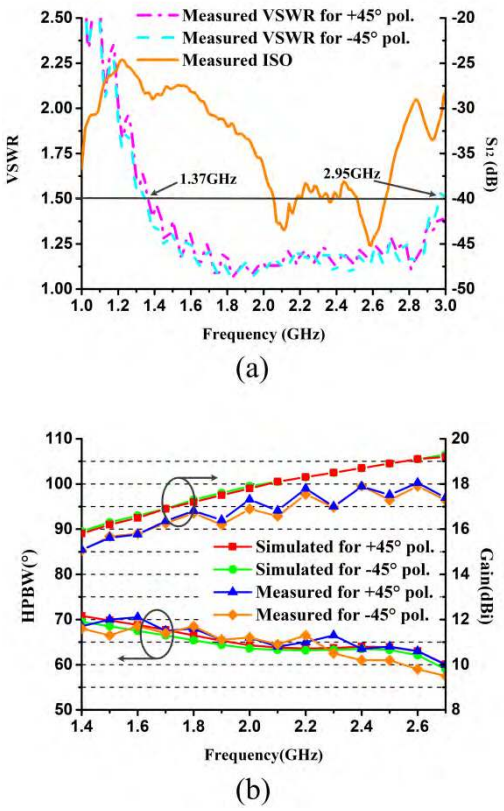

FIGURE 16. (a) Measured VSWR and ISO and (b) Measured and simulated gain and HPBW of the linear array.

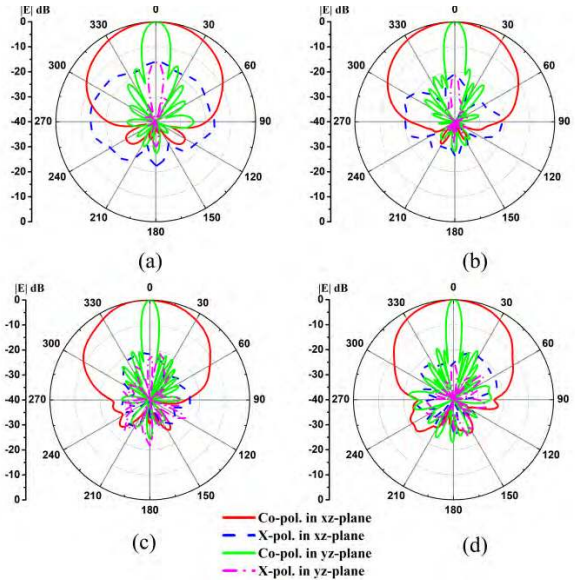

FIGURE 17. Measured radiation patterns of the linear array at (a) 1.42, (b) 1.9, (c) 2.4, and (d) 2.7 GHz.

eight-element array. The width of the reflector for the array is the same as that for the BEDPA.

As illustrated in Fig. 16(a), the linear array has a broad bandwidth of 73.1% (1.37 − 2.95 GHz) with the ISO > 27 dB. The measured gain and HPBW of the linear array with simulated results are shown in Fig. 16(b). It is found that the linear array achieves a gain within 16.5 ± 1.5 dBi, an HPBW within 64 ± 6.5°. The radiation patterns measured at 1.42, 1.9, 2.4 and 2.7 GHz for +45° polarization, as shown in Fig. 17. The BEDPA achieves a SLS > 16 dB and a front-to-back ratio (F/B) > 24dB. The proposed linear array exhibits high performance, which is important for commercial applications in AAU base station.

IV. CONCLUSION

The high-performance BEDPA with symmetrical open-resonant-slot pairs for 2/3/4G and IMT bands has been proposed. The BEDPA has achieved an enhanced bandwidth by etching symmetrical closed resonant slot on the conventional cross-dipole broadband dual-polarized antenna. The closed resonant slot has been successfully designed to be C-shaped, U-shaped and angular shaped. The BEDPA has obtained an impedance bandwidth of 67.3% (1.4 − 2.82 GHz) for VSWR < 1.5, while the conventional cross-dipole broadband dual-polarized antenna of 55.8% (1.42 − 2.52 GHz). Additionally, BEDPA has achieved a high ISO > 38 dB, a gain within 8.9 ± 0.7 dBi and an HPBW within 64.5 ± 4.5° throughout the operating frequency. The eight-element linear array has been fabricated and measured for AAU application. The linear array has achieved an impedance bandwidth of 73.1% (1.37 − 2.95 GHz) for VSWR < 1.5 with an ISO > 27 dB. The linear array has achieved a gain within 16.5 ± 1.5 dBi, a HPBW within 64 ± 6.5°, a SLS > 16 dB and a F/B > 24dB.

REFERENCES

[1] Y. Liu, H. Yi, F.-W. Wang, and S.-X. Gong, "A novel miniaturized broadband dual-polarized dipole antenna for base station," *IEEE Antennas Wireless Propag. Lett.*, vol. 12, pp. 1335–1338, 2013.

[2] Z. Bao, Z. Nie, and X. Zong, "A novel broadband dual-polarization antenna utilizing strong mutual coupling," *IEEE Trans. Antennas Propag.*, vol. 62, no. 1, pp. 450–454, Jan. 2014.

[3] Y. Cui, R. Li, and H. Fu, "A broadband dual-polarized planar antenna for 2G/3G/LTE base stations," *IEEE Trans. Antennas Propag.*, vol. 62, no. 9, pp. 4836–4840, Sep. 2014.

[4] Q.-X. Chu, D.-L. Wen, and Y. Luo, "A broadband ±45° dual-polarized antenna with Y-shaped feeding lines," *IEEE Trans. Antennas Propag.*, vol. 63, no. 2, pp. 483–490, Feb. 2015.

[5] H. Huang, Y. Liu, and S. Gong, "A broadband dual-polarized base station antenna with sturdy construction," *IEEE Antennas Wireless Propag. Lett.*, vol. 16, pp. 665–668, 2017.

[6] H. Sun, C. Ding, B. Jones, and Y. J. Guo, "A wideband base station antenna element with stable radiation pattern and reduced beam squint," *IEEE Access*, vol. 5, pp. 23022–23031, 2017.

[7] D.-Z. Zheng and Q.-X. Chu, "A wideband dual-polarized antenna with two independently controllable resonant modes and its array for base-station applications," *IEEE Antennas Wireless Propag. Lett.*, vol. 16, pp. 2014–2017, 2017.

[8] Y. Cui, R. Li, and P. Wang, "A novel broadband planar antenna for 2G/3G/LTE base stations," *IEEE Trans. Antennas Propag.*, vol. 61, no. 5, pp. 2767–2774, May 2013.

[9] Y. Gou, S. Yang, J. Li, and Z. Nie, "A compact dual-polarized printed dipole antenna with high isolation for wideband base station applications," *IEEE Trans. Antennas Propag.*, vol. 62, no. 8, pp. 4392–4395, Aug. 2014.

[10] W. Yu, Z. Zhang, A. Zhang, and X. Wu, "A broadband dual-polarized magneto-electric dipole antenna for 2G/3G/LTE applications," in *Proc. 6th Asia–Pacific Conf. Antennas Propag. (APCAP)*, 2017, pp. 1–3.

[11] C. Ding, H.-H. Sun, R. W. Ziolkowski, and Y. J. Guo, "A dual layered loop array antenna for base stations with enhanced cross-polarization discrimination," *IEEE Trans. Antennas Propag.*, vol. 66, no. 12, pp. 6975–6985, Dec. 2018.

[12] L.-H. Wen, S. Gao, Q. Luo, C.-X. Mao, W. Hu, Y. Yin, Y. Zhou, and Q. Wang, "Compact dual-polarized shared-dipole antennas for base station applications," *IEEE Trans. Antennas Propag.*, vol. 66, no. 12, pp. 6826–6834, Dec. 2018.
[13] Y. Cui, L. Wu, and R. Li, "Bandwidth enhancement of a broadband dual-polarized antenna for 2G/3G/4G and IMT base stations," *IEEE Trans. Antennas Propag.*, vol. 66, no. 12, pp. 7368–7373, Dec. 2018.
[14] Q. Zhang and Y. Gao, "A compact broadband dual-polarized antenna array for base stations," *IEEE Antennas Wireless Propag. Lett.*, vol. 17, no. 6, pp. 1073–1076, Jun. 2018.
[15] L. Wu, R. Li, Y. Qin, and Y. Cui, "Bandwidth-enhanced broadband dual-polarized antennas for 2G/3G/4G and IMT services," *IEEE Antennas Wireless Propag. Lett.*, vol. 17, no. 9, pp. 1702–1706, Sep. 2018.
[16] K. Chung, J. Kim, and J. Choi, "Wideband microstrip-fed monopole antenna having frequency band-notch function," *IEEE Microw. Wireless Compon. Lett.*, vol. 15, no. 11, pp. 766–768, Nov. 2005.
[17] Y. Chen, W. Lin, S. Li, and A. Raza, "A broadband ±45° dual-polarized multidipole antenna fed by capacitive coupling," *IEEE Trans. Antennas Propag.*, vol. 66, no. 5, pp. 2644–2649, May 2018.
[18] S. Zhong, *Antenna Theory and Techniques*. Beijing, China: Publishing House of Electronics Industry, 2011, pp. 94–248.
[19] S.-W. Wong, G.-H. Sun, L. Zhu, and Q.-X. Chu, "Broadband dual-polarization and stable-beamwidth slot antenna fed by U-shape microstrip line," *IEEE Trans. Antennas. Propag.*, vol. 64, no. 10, pp. 4477–4481, Oct. 2016.

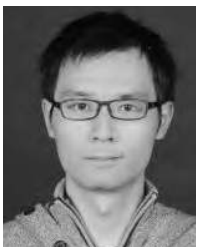

SUIDAO FU was born in Jiangsu, China, in 1990. He received the B.E. degree in electronic information science and technology from the Nanjing University of Aeronautics and Astronautics, Nanjing, China, in 2013, and the M.S. degree in electronics and communication engineering from Southeast University, Nanjing, in 2016, where he is currently pursuing the Ph.D. degree.

His current research interests include dual-polarized antennas, navigation antennas, and space–time adaptive anti-jamming process.

ZHENXIN CAO was born in 1976. He received the M.S. degree from the Nanjing University of Aeronautics and Astronautics, China, in 2002, and the Ph.D. degree from the School of Information Science and Engineering, Southeast University, China, in 2005.

From 2012 to 2013, he was a Visiting Scholar with North Carolina State University. Since 2005, he has been with the State Key Laboratory of Millimeter Waves, Southeast University, where he is currently a Professor. His research interest includes antenna theory and its applications.

PENG CHEN was born in Jiangsu, China, in 1989. He received the B.E. and Ph.D. degrees from the School of Information Science and Engineering, Southeast University, China, in 2011 and 2017, respectively, where he is currently an Associate Professor with the State Key Laboratory of Millimeter Waves.

From 2015 to 2016, he was a Visiting Scholar with the Electrical Engineering Department, Columbia University, New York, NY, USA. His research interests include radar signal processing and millimeter wave communication.

DI GAO was born in Shandong, China, in 1994. She received the bachelor's degree in applied physics from Xidian University, Xi'an, China, in 2015. She is currently pursuing the Ph.D. degree in electromagnetic field and microwave technology with Southeast University, Nanjing, China.

Her current research interests include phased-array antennas and base station antennas.

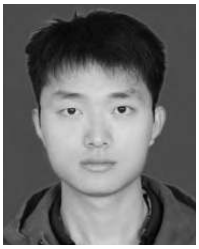

XIN QUAN was born in Henan, China, in 1993. He received the bachelor's degree in electronic information science and technology from the Nanjing University of Aeronautics and Astronautics, Nanjing, China, in 2015. He is currently pursuing the Ph.D. degree in electromagnetic field and microwave technology with Southeast University, Nanjing.

His current research interests include phased-array antennas and base station antennas.